



In-depth molecular analysis of combined and co-primary pulmonary large cell neuroendocrine carcinoma and adenocarcinoma

Bregtje C. M. Hermans^{1,2}  | Jules L. Derks^{1,2} | Lisa M. Hillen^{2,3} | Irene van der Baan^{2,3} | Esther C. van den Broek⁴ | Jan H. von der Thüsen⁵ | Robert-Jan van Suylen⁶ | Peggy N. Atmodimedjo⁵ | T. Dorine den Toom⁵ | Cecile Coumans-Stallinga^{2,3} | Wim Timens⁷ | Winand N. M. Dinjens⁵ | Hendrikus J. Dubbink⁵ | Ernst-Jan M. Speel^{2,3} | Anne-Marie C. Dingemans^{1,2,8}  | PALGA-group

¹Department of Pulmonary Diseases, Maastricht University Medical Centre+, Maastricht, The Netherlands

²GROW—School for Oncology & Developmental Biology, Maastricht University, Maastricht, The Netherlands

³Department of Pathology, Maastricht University Medical Centre+, Maastricht, The Netherlands

⁴PALGA Foundation, Houten, The Netherlands

⁵Department of Pathology, Erasmus MC Cancer Institute, University Medical Center Rotterdam, Rotterdam, The Netherlands

⁶Pathology-DNA, Location Jeroen Bosch Hospital, 's-Hertogenbosch, The Netherlands

⁷Department of Pathology and Medical Biology, University of Groningen, University Medical Center Groningen, Groningen, The Netherlands

⁸Department of Pulmonology, Erasmus MC Cancer Institute, University Medical Center Rotterdam, Rotterdam, The Netherlands

Correspondence

Anne-Marie C. Dingemans, Department of Pulmonology, Erasmus MC Cancer Institute, University Medical Center Rotterdam, P.O. Box 2040, 3000 CA Rotterdam, The Netherlands.
Email: a.dingemans@erasmusmc.nl

Abstract

Up to 14% of large cell neuroendocrine carcinomas (LCNECs) are diagnosed in continuity with nonsmall cell lung carcinoma. In addition to these combined lesions, 1% to 7% of lung tumors present as co-primary tumors with multiple synchronous lesions. We evaluated molecular and clinicopathological characteristics of combined and co-primary LCNEC-adenocarcinoma (ADC) tumors. Ten patients with LCNEC-ADC (combined) and five patients with multiple synchronous ipsilateral LCNEC and ADC tumors (co-primary) were included. DNA was isolated from distinct tumor parts, and 65 cancer genes were analyzed by next generation sequencing. Immunohistochemistry was performed including neuroendocrine markers, pRb, Ascl1 and Rest. Pure ADC (N = 37) and LCNEC (N = 17)

Abbreviations: 95% CI, 95% confidence interval; ADC, adenocarcinoma; CNV, copy number variation; FISH, fluorescence in situ hybridization; HE slides, hematoxylin-eosin slides; IHC, immunohistochemistry; LCNEC, large cell neuroendocrine carcinoma; NSCLC, nonsmall cell lung carcinoma; OS, overall survival; SCLC, small cell lung carcinoma; SNP, single nucleotide polymorphism; TKIs, tyrosine kinase inhibitors; TMA, tissue micro arrays.

Ernst-Jan M. Speel and Anne-Marie C. Dingemans contributed equally to this work.

PALGA-group participating investigators: J.E. Broers: Isala Klinieken (Zwolle); C.M. van Dish: Klinische Pathologie Groene Hart Ziekenhuis (Gouda); M.C.H. Hogenes: Labpon (Hengelo); J.C.C. van der Meij: Pathologie Friesland (Leeuwarden); J.W.R. Meijer: Ziekenhuis Rijnstate (Arnhem); F.H. van Nederveen: Laboratorium voor Pathologie (PAL) (Dordrecht); E.W.P. Nijhuis: Onze Lieve Vrouwe Gasthuis (Amsterdam); T. Radonic: Amsterdam Universitair Medisch Centrum (Vrije Universiteit) (Amsterdam); NN: Radboud UMC (Nijmegen).

This is an open access article under the terms of the Creative Commons Attribution-NonCommercial-NoDerivs License, which permits use and distribution in any medium, provided the original work is properly cited, the use is non-commercial and no modifications or adaptations are made.

© 2021 The Authors. *International Journal of Cancer* published by John Wiley & Sons Ltd on behalf of UICC.

cases were used for reference. At least 1 shared mutation, indicating tumor clonality, was found in LCNEC- and ADC-parts of 10/10 combined tumors but only in 1/5 co-primary tumors. A range of identical mutations was observed in both parts of combined tumors: 8/10 contained ADC-related (*EGFR/KRAS/STK11* and/or *KEAP1*), 4/10 *RB1* and 9/10 *TP53* mutations. Loss of pRb IHC was observed in 6/10 LCNEC- and 4/10 ADC-parts. The number and intensity of expression of *Ascl1* and neuroendocrine markers increased from pure ADC (low) to combined ADC (intermediate) and combined and pure LCNEC (high). The opposite was true for *Rest* expression. In conclusion, all combined LCNEC-ADC tumors were clonally related indicating a common origin. A relatively high frequency of pRb inactivation was observed in both LCNEC- and ADC-parts, suggesting an underlying role in LCNEC-ADC development. Furthermore, neuroendocrine differentiation might be modulated by *Ascl1*(+) and *Rest*(-) expression.

KEYWORDS

Ascl1, LCNEC, pRb, *RB1*, *Rest*

What's new?

Large cell neuroendocrine carcinoma (LCNEC) is a rare malignancy in which about 14 percent of tumors are diagnosed in continuity with lung adenocarcinoma (ADC) or squamous cell carcinoma. Here, to better understand tumorigenesis of LCNEC, e.g. by ADC transformation, the authors analyzed molecular and clinicopathological characteristics of LCNEC-ADC tumors. Tumors with combined LCNEC- and ADC-parts were found to be clonally related and frequently carried mutations known to occur in pure ADC, with high rates of pRb inactivation linked to neuroendocrine differentiation. By contrast, co-primary LCNEC and ADC tumors were not often clonally related, suggesting that such tumors should be considered as distinct primary lesions rather than metastatic disease.

1 | INTRODUCTION

Adenocarcinoma (ADC) is the most common type of lung cancer, and oncogenesis is often driven by well-known mutually exclusive oncogenes, for example, *KRAS* and *EGFR*.^{1,2} In the last decades, tyrosine kinase inhibitors (TKIs) have been developed to target those oncogenes. Survival rates of stage-IV disease have significantly been improved applying these new therapies. Resistance mechanisms to TKIs include additional mutations in the driver gene, the downstream signaling pathway, bypass signaling pathways, or transformation to small cell lung carcinoma (SCLC) or, less frequently, large cell neuroendocrine carcinoma (LCNEC).³⁻⁸ The two latter mechanisms are associated with *RB1* mutations in addition to *TP53* mutations.^{5,6,9,10}

LCNEC is a rare pulmonary tumor, accounting for 1% to 3% of all lung carcinoma.¹¹⁻¹⁴ LCNEC is characterized by neuroendocrine morphology and positive immunohistochemical (IHC) staining of at least one neuroendocrine marker (*Cd56*, *Chromogranin A* and/or *Synaptophysin*).¹⁴ Besides the before mentioned transformation of ADC to LCNEC, other pathways of LCNEC oncogenesis are also involved. LCNEC seems to be a heterogeneous disease with clinically relevant subgroups.¹⁵⁻¹⁷ Almost half of LCNECs are mutated in both *TP53* and *RB1*, and since this is a feature of SCLC, this is called the SCLC-like subtype.¹⁵⁻¹⁷ Another part of LCNECs

harbor mutations in oncogenes identified in nonsmall cell lung carcinoma (NSCLC), for example, *KEAP1*, *STK11*, *EGFR* or *KRAS*, often in combination with *TP53* mutations (NSCLC-like subtype).¹⁵⁻¹⁷

Interestingly, some LCNECs are combined with morphologically separate areas of ADC and/or squamous cell carcinoma, reported in up to 14% of LCNEC.¹⁸⁻²⁰ The two morphological distinct parts, one with clear neuroendocrine morphology, distinguish those combined tumors from NSCLC with neuroendocrine differentiation (NSCLC morphology with expression of neuroendocrine markers). Combined tumors may evolve due to a collision of two separate tumor nodules.^{21,22} Alternatively, the combined tumor might be the result of transformation of ADC toward neuroendocrine carcinoma in part of the tumor, in analogy to neuroendocrine transformation after TKI treatment, or vice versa.^{5,6} A combined tumor might also be the result of two divergent differentiation lineages of a tumor stem cell. This divergence might take place early in tumorigenesis or as a late event, resulting in a high overlap of mutations in both tumor parts. A clonal relationship between the two lesions has been shown for transformed tumors due to TKI treatment and for combined SCLC-NSCLC tumors, but has not adequately been investigated between neuroendocrine and nonneuroendocrine regions of combined LCNEC-NSCLC tumors.^{5,6,23-25}

In addition, some lung cancer patients have two or more synchronous ipsilateral pulmonary lesions at diagnosis. Such lesions might be metastases of the primary tumor or a second independent primary tumor. Incidence of such co-primary lung tumors has been reported to be 1% to 7% in surgical series and up to 16% in more recent and unselected series.^{22,26-32} Only limited reports on LCNEC as part of co-primary ipsilateral lung tumors are available.³²⁻³⁴ According to current guidelines, two lung lesions with a different histologic subtype should be regarded as independent primary tumors.³⁵ However, some studies have shown clonality between multiple lesions with different histologic NSCLC subtypes, indicating that a common origin cannot be excluded.^{36,37}

In our study, we performed an in-depth analysis of molecular, neuroendocrine and clinicopathological characteristics of 10 combined LCNEC-ADC tumors. Furthermore, we analyzed the characteristics of five ipsilateral synchronous pulmonary lesions, including at least one single tumor nodule with LCNEC.

2 | MATERIALS AND METHODS

2.1 | Sample selection

Pathology reports of patients with LCNEC diagnosed in the Netherlands between 2003 and 2012 were retrieved from PALGA, the nationwide network and registry of histo- and cytopathology in the Netherlands (Figure S1).^{11,38} All reports were assessed by two researchers (B.H. and J.D.). All resection specimens containing both LCNEC and ADC morphology in one sample were identified for the “combined LCNEC” group. Samples with positive neuroendocrine IHC markers but exclusively ADC morphology were regarded as NSCLC with neuroendocrine differentiation and not included in our study. All cases with two resected synchronous ipsilateral pulmonary lesions, one being (partly) LCNEC and one being ADC, were selected for the “co-primary tumor” group. Central revision by three experienced lung pathologists (R.v.S, L.H. and J.v.d.T.) was performed for those samples. Only samples with the LCNEC-part fulfilling the WHO-classification criteria (2015) for LCNEC (ie, neuroendocrine morphology and at least one neuroendocrine marker with $\geq 10\%$ staining) and the ADC-part for ADC were included.¹⁴ Furthermore, the two parts had to be adequately distinguishable, and both parts should comprise a substantial percentage of the total tumor (ie, $\geq 10\%$). Patients who had received neo-adjuvant chemotherapy were excluded.

2.2 | DNA isolation

For each sample, four 10 μm slides were cut from a formalin-fixed paraffin-embedded (FFPE) block for DNA isolation, and before and after a 4 μm slide was cut for hematoxylin-eosin (HE) staining. Two experienced pulmonary pathologists (L.H. and J.v.d.T.) marked LCNEC- and ADC-parts on those HE slides and estimated tumor cell percentages (minimally 30%). The 10 μm slides were hematoxylin stained, and manual micro-dissection was performed under a dissecting microscope. Selected parts with maximum

distance between the two parts were dissected, to avoid dissection from any transition area (Figure S2). The dissected tissue fragments were incubated overnight at 56°C in 5% Chelex (Chelex 100 Resin [BioRad] in lysis buffer solution [Promega]) and 20 mg/mL proteinase K, mixed in a ratio 10:1. Next, the samples were incubated for 10 minutes at 95°C, and after centrifuging, the supernatant was collected.

2.3 | Mutational and copy number variation analysis

Targeted next generation sequencing was performed by semiconductor sequencing with the Ion Torrent platform using the supplier's materials and protocols (Thermo Fisher Scientific) with a custom-made dedicated panel for mutational analysis (65 genes), including genes frequently mutated in ADC (*EGFR*, *KRAS*, *BRAF* and *ALK* [mutation hotspots]) and LCNEC (*RB1* [coding coverage 99%], *TP53* [100%], *KEAP1* [100%], *STK11* [100%] and *NOTCH1* [exon 26 and 27]) (Supplemental Methods). In addition, the panel comprised 262 highly polymorphic single nucleotide polymorphism (SNP) amplicons for copy number variation (CNV) detection (chromosomes: 1p, 2p, 3p, 5q, 6p, 7p, 8p, 9p, 10q, 11q, 12q, 13q, 15q, 16q, 17p, 18q, 19p and Xp).³⁹ Library and template preparations were performed consecutively with the AmpliSeq Library Kit 2.0-384 LV and the Ion 540 Chef kit. Sequencing was performed on a 540 chip with the Ion GeneStudio S5XL system. Data were analyzed with Sequence Pilot Analysis Software (JSI Medical Systems). For each patient, normal tissue was included as a reference. For quality control, only variants with an amplicon coverage of >100 were taken into account. DNA variants, which were also present in normal tissue, were regarded as polymorphisms. CNV (ie, amplifications, gains and deletions) was analyzed by normalized coverage using the Sequence Pilot Analysis Software. Homozygous deletions of *RB1* were confirmed by fluorescence in situ hybridization (FISH). In addition, more sensitive SNP-based CNV analysis was performed as described earlier.³⁹

2.4 | Immunohistochemistry

Automated IHC staining for p53, pRb, Ascl1, Rest, NeuroD1, Cd56, Chromogranin A, Synaptophysin, Sox1 and Ki-67 was performed for all samples on 4 μm tissue sections on coated glass slides with the DAKO auto stainer (Agilent, Santa Clara, CA). A list of antibodies with dilution and information on the protocol (pH antigen retrieval and use of linkers) is provided in Table S1. Tissue micro arrays (TMAs) with material from resected confirmed pure ADC (N = 37) and resected confirmed pure LCNEC (N = 17) were used as a reference.

Protein expression was assessed for percentage of positive tumor cells (0%-100%) and staining intensity (0, 1, 2 or 3) by B. H., J. D. and J. v. d. T. H-scores were calculated by multiplying percentage of positive tumor cells by intensity. Ki-67 proliferation index was assessed by eyeball estimation by J.v.d.T. Type of staining (membranous, cytoplasmic or membranous) and cut-off values for the different antibodies are shown in Table S1.

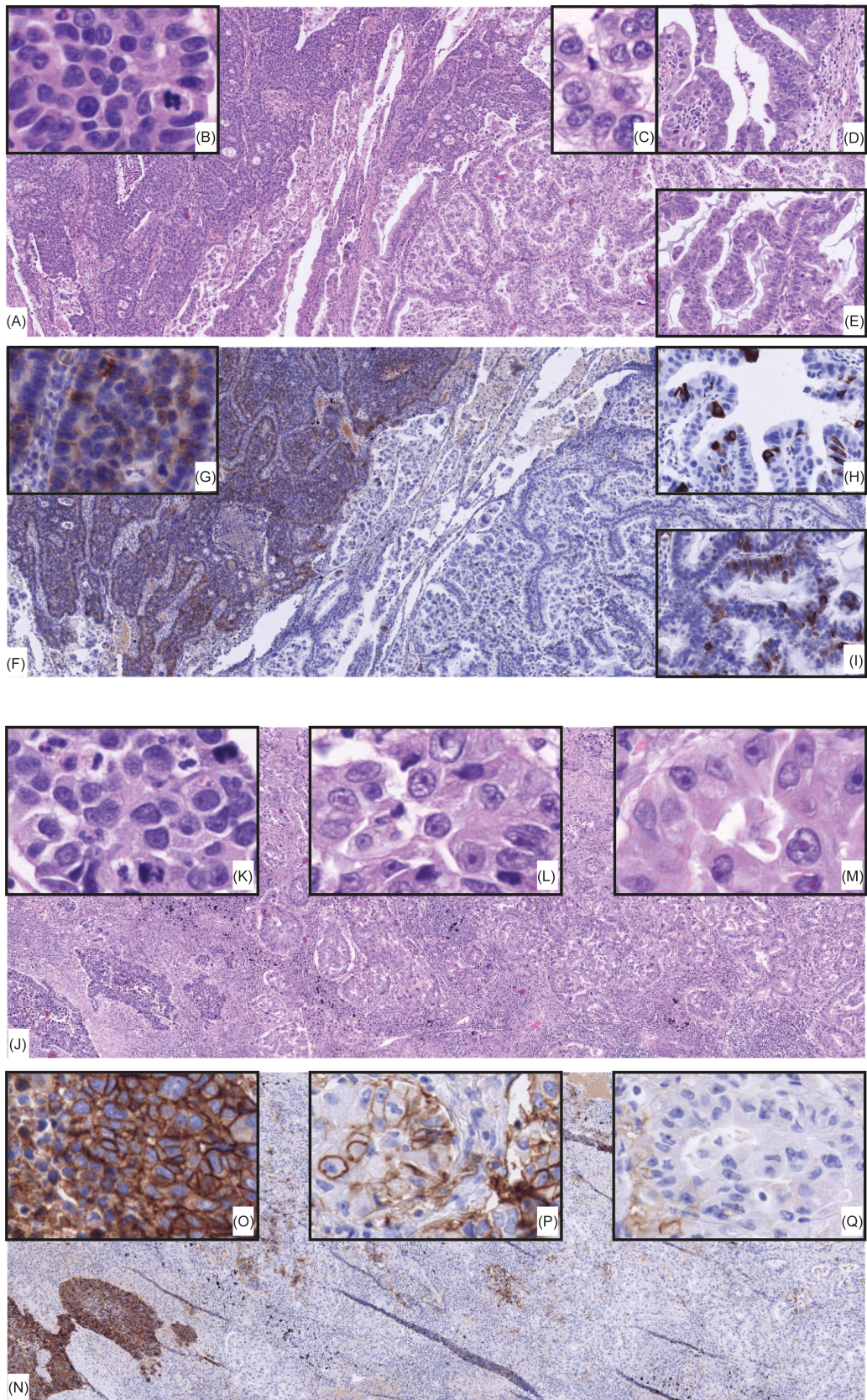


FIGURE 1 Legend on next page.

FIGURE 1 Representative cases of combined large cell neuroendocrine carcinoma (LCNEC)-adenocarcinoma (ADC) tumors. (A) Hematoxylin-eosin (HE) staining (magnification ×40) of LCNEC (left) and ADC (right) with a clear border between the two parts and no transition zone (Patient 4). (B) Detailed HE staining of LCNEC-part (magnification ×400). (C-E) Detailed HE stainings of ADC-part (magnification [C] ×400 and [D,E] ×100). (F) Overview of Cd56 immunohistochemical staining (magnification ×40) in the same tumor as (A) with high expression in LCNEC-part and low expression in ADC-part. (G) Detailed Cd56 immunohistochemical staining (magnification ×200) in LCNEC-part. (H) Detailed synaptophysin immunohistochemical staining in ADC-part with scattered increased single cell expression (magnification ×100). (I) Detailed Cd56 immunohistochemical staining in ADC-part with membranous and cytoplasmic staining of single cells or clusters of cells (magnification ×100). (J) HE staining (magnification ×40) of LCNEC (left), transition zone (middle) and ADC (right) (Patient 3). (K) Detailed HE staining of LCNEC-part (magnification ×400). (L) Detailed HE staining of transition zone (magnification ×400). (M) Detailed HE staining of ADC-part (magnification ×400). (N) Cd56 immunohistochemical staining (magnification ×40) with high expression in LCNEC-part (left), intermediate expression in transition zone (middle) and low expression in ADC-part (right). (O-Q) Detailed Cd56 immunohistochemical stainings (magnification ×200) in LCNEC-part (O), transition zone (P) and ADC-part (Q)

(A)

	Patient 2		Patient 4		Patient 14		Patient 3		Patient 13		Patient 1		Patient 7		Patient 9		Patient 5		Patient 8		
	ADC	LCNEC	ADC	LCNEC	ADC	LCNEC	ADC	LCNEC	ADC	LCNEC	ADC	LCNEC	ADC	LCNEC	ADC	LCNEC	ADC	LCNEC	ADC	LCNEC	
Mutations																					
TP53																					
RB1																					
KEAP1																					
STK11																					
KRAS																					
EGFR																					
IGF1R																					
MTOR																					
CDKN2A																					
ARID1A																					
CCNE1																					
PIK3CA																					
POLE																					
PTEN																					
RET																					
IHC																					
p53	-	-	-	-	-	-	++	++	-	-	++	++	-	-	-	-	++	++	-	-	
pRb	+	+	+	+	+	+	+	-	-	-	-	-	-	-	-	+	+	+	+	-	
Ascl1	-	+	+	+	++	++	-	+	-	+	+	++	-	+	-	+	-	+	+	++	
Rest	++	+	+	+	++	++	+	+	+	+	+	+	+	+	++	+	+	+	+	-	
NeuroD1	++	+	+	+	++	++	+	+	+	+	+	+	+	+	++	+	+	++	-	-	
Cd56	-	-	+	++	+	+	+	++	-	-	+	++	-	++	-	-	+	+	+	+	
ChrmA	-	++	+	+	-	-	-	-	-	++	+	-	-	-	-	+	-	+	+	+	
Syn	-	++	+	+	++	++	+	+	-	++	+	+	-	+	-	++	-	++	-	+	
Ttf1	++	+	++	++	++	++	++	++	++	++	++	++	++	++	++	++	++	++	++	++	
Sox1	+	-	-	-	-	-	+	+	-	-	+	+	-	-	+	+	+	+	+	+	
Ki-67	15	40	50	50	50	70	20	20	10	50	60	100	30	40	30	30	15	50	50	80	
Type ¹	NSCLC-like				NSCLC-like with RB1 mut/pRb loss								SCLC-like								
Clinical																					
Gender	F	M	M	M	F	M	F	M	F	M	F	M	F	M	F	M	F	M	F	M	
Age	61	60	52	67	72	58	42	71	69	68											
Stage	IA	IIIA	IA	IIIA	IIIA	IV ²	IV ²	IA	IV ²	IA											
Treatment	Lob	Lob + CTx	Lob	Lob	Lob + CTx	Lob + CTx	Lob + CTx	Lob	Unknown	Lob											
Survival (months)	68	31	20	31	19	105+	33	86+	29	75											

Mutational analysis		Immunohistochemical staining	
Missense		-	H-score 0
Nonsense		+	H-score ≥1-150
Splice		++	H-score ≥151-300
Frameshift		p53 -	Loss
In frame deletion		p53 ++	Upregulation
Not in database ³			IHC not available

¹LCNEC part of the tumor: NSCLC-like = RB1 wildtype and preserved pRb IHC expression; NSCLC-like with RB1 mut/pRb loss = NSCLC-like mutations (ie, STK11, KEAP1, EGFR) in combination with RB1 mutation or pRb loss; SCLC-like = pRb loss and/or RB1 mutation without mutations in STK11, KEAP1 or EGFR. ²Lung or pleural metastases. ³International Agency for Research on Cancer (IARC) TP53 database

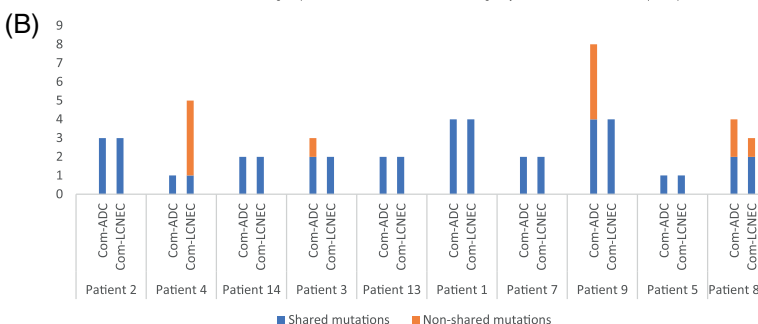








FIGURE 2 Combined large cell neuroendocrine carcinoma and adenocarcinoma. (A) Type of mutations, immunohistochemical staining and clinical characteristics in LCNEC-parts and ADC-parts. In all tumors with the same type of mutation in both tumor parts, this was a shared mutation. (B) Number of shared and nonshared mutations between LCNEC-parts and ADC-parts. A, amplification; ADC, adenocarcinoma; ChrmA, Chromogranin A; com-ADC, combined tumor, ADC-part; com-LCNEC, combined tumor, LCNEC-part; CTx, adjuvant chemotherapy; F, female; HD, homozygous deletion; IHC, immunohistochemistry; LCNEC, large cell neuroendocrine carcinoma; lob, lobectomy; M, male; Syn, Synaptophysin [Color figure can be viewed at wileyonlinelibrary.com]

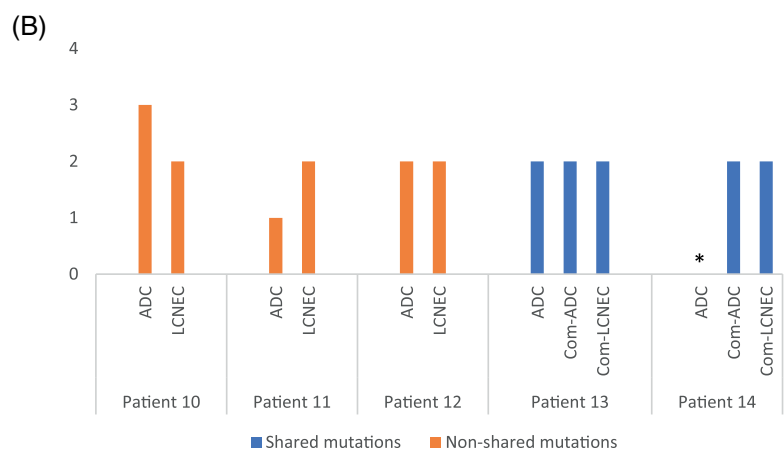
FIGURE 3 Co-primary large cell neuroendocrine carcinoma and adenocarcinoma, including two patients with combined large cell neuroendocrine carcinoma-adenocarcinoma and co-primary adenocarcinoma (Patients 13 and 14). (A) Type of mutations and outcome of immunohistochemical staining and clinical characteristics in LCNEC and ADC. (B) Number of shared and nonshared mutations between LCNEC and ADC. *No mutations were found in co-primary ADC lesion of Patient 14. A, amplification; ADC, adenocarcinoma; bilob, bilobectomy; ChrmA, Chromogranin A; com-ADC, combined tumor, ADC-part; com-LCNEC, combined tumor, LCNEC-part; CTx, adjuvant chemotherapy; F, female; G, gain; HD, homozygous deletion; IHC, immunohistochemistry; LCNEC, large cell neuroendocrine carcinoma; lob, lobectomy; M, male; PA, partial amplification; sublob, sublobectomy; Syn, Synaptophysin [Color figure can be viewed at wileyonlinelibrary.com]

(A)

	Patient 10		Patient 11		Patient 12		Patient 13			Patient 14		
	ADC	LCNEC	ADC	LCNEC	ADC	LCNEC	ADC	Com-ADC	Com-LCNEC	ADC	Com-ADC	Com-LCNEC
Mutations												
<i>TP53</i>												
<i>RB1</i>												
<i>KEAP1</i>												
<i>STK11</i>												
<i>KRAS</i>												
<i>PIK3CA</i>												
<i>KIT</i>												
<i>CCND1</i>												
<i>ERBB2</i>	A	?	PA									
IHC												
p53							-	-	-	+	-	-
pRb							+	-	-	+	+	+
Ascl1							+	-	+	+	++	++
Rest							+	+	+	+	+	+
Cd56							-	-	+	-	+	+
ChrmA							-	-	++	-	-	-
Syn							-	-	++	-	++	+
Ttf1							++	++	++	++	++	++
Sox1							-	-	-	-	-	-
Ki-67							15	10	50	-	50	70
Clinical												
Gender	M		M		M		F					M
Age	69		62		74		72					52
Stage	IA		IIIB		IB		IIIA					IA
Treatment	Sublob		Bilob + CTx		Sublob		Lob + CTx					Lob
Survival (months)	35		53		23		19					20

Mutational analysis		Immunohistochemical staining	
	Missense	-	H-score 0
	Nonsense	+	H-score ≥1-150
	Splice	++	H-score ≥151-300
	Frameshift	p53 -	Loss
	In frame deletion	p53 +	Wildtype expression
	Not in database*	p53 ++	Upregulation
			IHC not available

* International Agency for Research on Cancer (IARC) TP53 database



2.5 | Statistical analysis

All analyses were performed using SPSS (version 25 for Windows, Armonk, New York: IBM Corp.). Patient characteristics were analyzed with descriptive statistics. Median overall survival (OS) was estimated with Kaplan-Meier analysis and is presented with a 95% confidence interval (95% CI).

For each IHC marker, expression in the four histological subtypes (pure ADC, combined tumor ADC-part, combined tumor LCNEC-part and pure LCNEC) is reported, and associations between histology and IHC marker expression were evaluated with chi-square or Fisher's exact test, followed by multiple post hoc tests if appropriate. Median H-scores were calculated for all IHC markers in the four different histologic groups. Differences in H-scores between the histologic subgroups were tested with

Kruskal-Wallis Test followed by multiple post hoc Mann-Whitney *U* tests, if appropriate. *P* values <.05 were considered significant.

3 | RESULTS

3.1 | Patient selection and pathological review

Screening of 305 LCNEC pathology reports identified 27 LCNEC with combined and/or a co-primary LCNEC-ADC diagnosis. After pathological review, combined LCNEC-ADC morphology was confirmed in eight patients, combined LCNEC-ADC with an ADC co-primary tumor in two patients and co-primary LCNEC and ADC tumors in three patients. These 13 unique patients were included

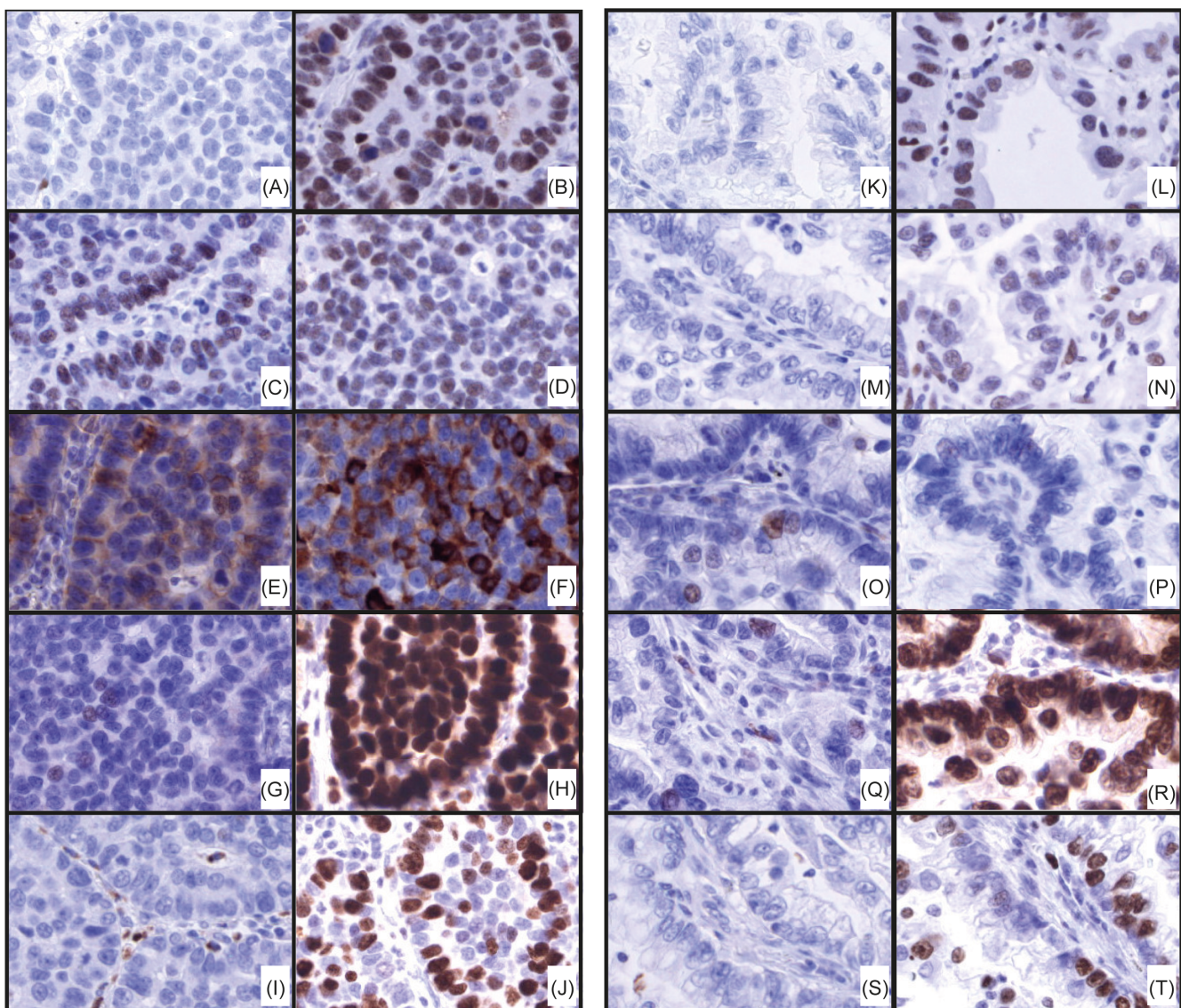


FIGURE 4 Examples of immunohistochemical stainings (magnification $\times 200$) in the combined large cell neuroendocrine carcinoma-adenocarcinoma of Patient 4. (A-J) Immunohistochemical stainings in LCNEC-part: (A) p53, (B) pRb, (C) Ascl1, (D) Rest, (E) Cd56 (Figure 1G reused), (F) Synaptophysin, (G) Chromogranin A, (H) Ttf1, (I) Sox1 and (J) Ki-67. (K-T) Immunohistochemical stainings in ADC-part: (K) p53, (L) pRb, (M) Ascl1, (N) Rest, (O) Cd56, (P) Synaptophysin, (Q) Chromogranin A, (R) Ttf1, (S) Sox1 and (T) Ki-67

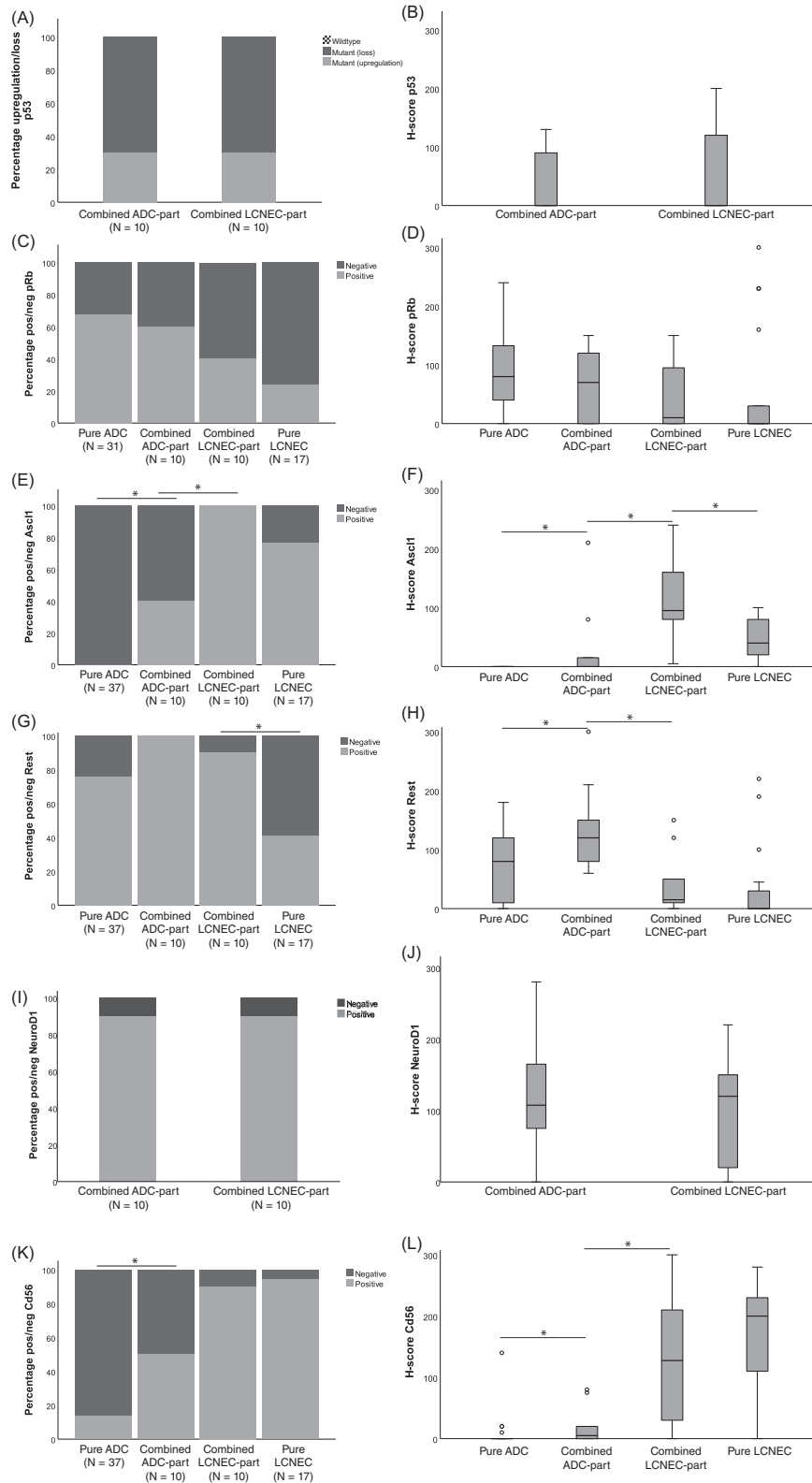


FIGURE 5 Results of immunohistochemical staining, presented by positive/negative staining and H-score for (A,B) p53, (C,D) pRb, (E,F) Ascl1, (G,H) Rest, (I,J) NeuroD1, (K,L) Cd56, (M,N) Synaptophysin, (O,P) Chromogranin A, (Q,R) Ttf1, (S,T) Sox1 and (U) percentage of positive tumor cells after Ki-67 staining

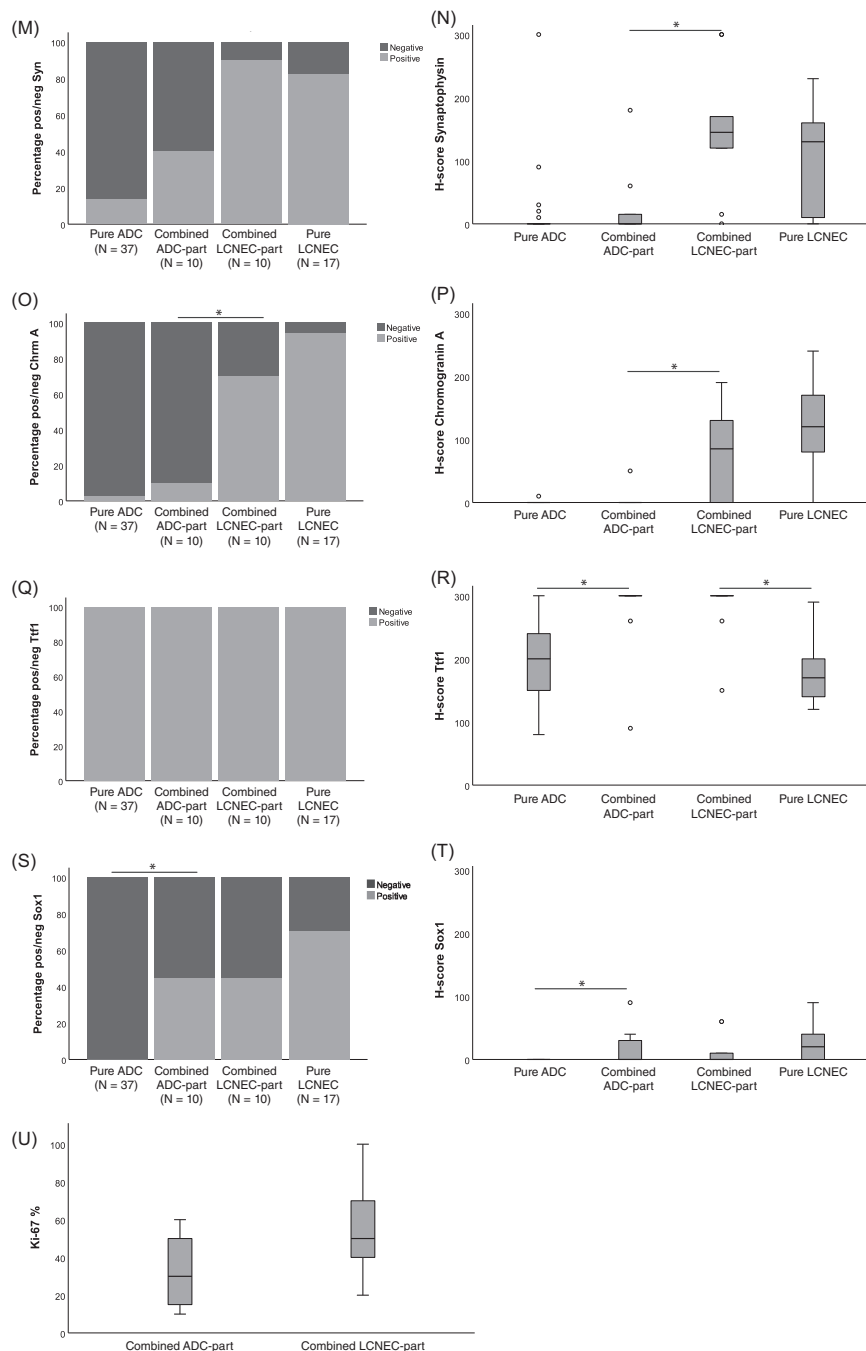


FIGURE 5 (Continued)

in the combined LCNEC-ADC group (N = 10, 3%) and/or the group with co-primary synchronous ipsilateral LCNEC and ADC tumors (N = 5, 2%) (Figure S1). In all combined tumors, clearly distinguishable parts of both LCNEC and ADC were identified (Figure 1). In some of the tumors, a transition area with characteristics of both LCNEC and ADC was also present (Figure 1). Patient characteristics are presented in Figures 2A and 3A. Median OS was 31 months (95% CI 27-35 months) in the combined tumor group and 23 months (95% CI 17-29 months) in the co-primary group.

3.2 | Mutational analysis

Tumor clonality was indicated by shared (non-hotspot) mutations in 10/10 combined LCNEC-ADC tumors, while only in 1/5 co-primary tumors, a clonal relation was confirmed using mutation and CNV analysis. These shared mutations were not found in the analyzed normal tissue of the respective patients, excluding germline mutations. At least two identical somatic mutations were found in 8/10 combined tumors with a median of 2 (range 1-4) mutations (Figure 2 and Table S2). Of all identified

TABLE 1 Overview of common mutations in pure LCNEC and in combined LCNEC-ADC

	Year	Patients	TP53	STK11	KEAP1	KRAS	EGFR	RB1	Loss of pRb IHC
Pure LCNEC									
Rekhtman et al ¹⁷	2016	N = 45	35/45 (78%)	15/45 (33%)	14/45 (31%)	10/45 (22%)	0/45 (0%)	17/45 (38%)	25/42 (60%)
Miyoshi et al ¹⁹	2017	N = 68	46/68 (68%)	NR	NR	4/68 (6%)	0/68 (0%)	18/68 (26%)	48/65 (74%)
Ito et al ⁴⁰	2017	N = 8	5/8 (63%)	0/8 (0%)	1/8 (13%)	1/8 (13%)	0/8 (0%)	2/8 (25%)	4/7 (57%)
George et al ¹⁶	2018	N = 46	41/46 (89%)	18/46 (39%)	13/46 (28%)	6/46 (13%) ^a	NR	15/46 (33%)	NR
Derks et al ^{15,46}	2018	N = 79	67/79 (85%)	8/79 (10%)	14/79 (18%)	NR	NR	37/79 (47%)	78/109 ^b (72%)
Milione ^c et al ⁴¹	2020	N = 34	25/34 (74%)	2/34 (6%)	NR	5/34 (15%)	0/34 (0%)	10/34 (29%)	45/70 ^b (64%)
Combined ADC-LCNEC									
Miyoshi et al ¹⁹	2017	N = 5	4/5 (80%)	NR	NR	1/5 (20%)	1/5 (20%)	1/5 (20%)	NR
Ito et al ⁴⁰	2017	N = 10	6/10 (60%)	0/10 (0%)	2/10 (20%)	1/10 (10%)	1/10 (10%)	4/10 (40%)	7/10 (70%)
Milione ^c et al ⁴¹	2020	N = 16	6/16 (38%)	0/16 (0%)	NR	6/16 (38%)	0/16 (0%)	1/16 (6%)	8/26 ^b (31%)
Our study		N = 10	9/10 (90%)	3/10 (30%)	3/10 (30%)	3/10 (30%)	1/10 (10%)	4/10 (40%) ^d	6/10 (60%)

Abbreviations: ADC, adenocarcinoma; IHC, immunohistochemistry; LCNEC, large cell neuroendocrine carcinoma, NR, not reported.

^aKRAS/NRAS/HRAS.

^bAdditional patients could be included for IHC compared to mutational analysis.

^cOnly hotspot mutations were analyzed, not covering all and/or complete exons. Therefore percentages of detected mutations may be lower.

^dIncluding one homozygous deletion.

mutations (N = 35) in the combined LCNEC-ADC tumors, N = 23 (66%) were identified in both parts. Commonly identified identical mutations in both combined tumor parts included mutations in *TP53* (90%), *RB1* (30%), *KEAP1* (30%), *STK11* (30%) and *KRAS* (30%). A total of N = 5 (14%) different mutations were unique to LCNEC-parts and N = 7 (20%) to ADC-parts. Furthermore, homozygous deletion of *RB1* (confirmed by FISH) was found in one patient in both the LCNEC- and ADC-parts, and amplification of *CCNE1* was found in the LCNEC-part of another patient (Figure 2). In the co-primary tumors, clonality was only demonstrated in a combined LCNEC-ADC with also a co-primary ADC (Patient 13). This patient had two identical somatic mutations in both the ADC-part and LCNEC-part of the combined lesion and the second ADC lesion. No clonal relation was established in the three patients with pure co-primary tumors as well as in the other combined LCNEC-ADC with co-primary ADC (Patient 14) (Figure 3 and Table S2). The sequencing coverage and quality statistics for each sample are summarized in Table S3.

3.3 | Immunohistochemical staining

IHC markers were evaluated in LCNEC- and ADC-parts of combined tumors (Figure 4) and pure LCNEC and ADC as a reference. All combined cases had a nonwildtype p53 staining pattern in both LCNEC- and ADC-parts, with upregulation in 3/10 cases and loss of p53 staining in 7/10 cases, in agreement with mutational analysis (Figure 2). In 4/10 combined cases, both LCNEC- and ADC-parts had loss of pRb expression, and *RB1* was inactivated in 3/4 of those cases (mutation or homozygous deletion). In two additional cases, pRb was only lost in the LCNEC-part, and the inactivation mechanism for *RB1* was not found (ie, no *RB1* mutations or homozygous deletion) (Figure 2). Evaluation of transcription factors regulating neuroendocrine differentiation showed upregulation for *Ascl1* and downregulation of *Rest* in LCNEC-parts of combined tumors and pure LCNEC, compared with expression in pure ADC and ADC-parts of the combined tumors (Figure 5 and Tables S4 and S5).

Expression of neuroendocrine markers was found in 10/10 LCNEC-parts and in 5/10 ADC-parts of combined tumors (Figure 2A). In the latter parts, a slightly increased expression for neuroendocrine markers was observed most closely to LCNEC-parts, or an increased neuroendocrine marker expression was found in single cells in the entire ADC-part (Figure 1). The number and intensity of positive neuroendocrine markers increased comparing pure ADC (low) with combined ADC (intermediate) and combined and pure LCNEC (high) (Figure 5 and Tables S4 and S5).

Ttf1 expression was positive in all cases, though a significantly lower median H-score was found in both pure ADC and pure LCNEC compared with their equivalents in the combined tumors (Figure 5 and Tables S4 and S5). For Sox1, a slight increase in positive cases and H-scores was observed in ADC-parts of combined tumors compared with pure ADC (Figure 5 and Tables S4 and S5). No differences

were found for NeuroD1 expression (Figure 5 and Tables S4 and S5). Median Ki-67 proliferation index was 30 in ADC-parts of combined tumors and 50 in LCNEC-parts ($P = .077$) (Figure 5 and Table S5).

4 | DISCUSSION

We present a unique cohort of 10 combined LCNEC-ADC tumors and show that both histological tumor parts are clonally related in all cases, whereas only one out of five synchronous ipsilateral LCNEC and ADC tumors was clonally related. Common mutations found in ADC (ie, *TP53/EGFR/KRAS/STK11* and *KEAP1*) as well as in SCLC and SCLC-like LCNEC (ie, *RB1* inactivation) were observed in both parts of combined LCNEC-ADC. The latter finding is of interest, because *RB1* mutations are frequently found in *EGFR* mutated ADC transforming into SCLC (and LCNEC) under TKI treatment.^{5,6,9,10} Hence, combined LCNEC-ADC may develop from a common cell of origin related to ADC, in which inactivation of genes such as *RB1* or dysregulation of *Ascl1(+)* and *Rest(-)* may promote neuroendocrine transformation.

An overview of available literature on commonly mutated genes in combined LCNEC-ADC and pure LCNEC is provided in Table 1.^{15-17,19,40,41} Similar to LCNEC, almost all combined LCNEC-ADC harbor *TP53* mutations.^{15-17,19,40} Furthermore, other mutations related to ADC were found in 8/10 patients in our study. Especially, *KRAS* and *EGFR* mutations occur more frequently in combined LCNEC-ADC tumors compared with pure LCNEC tumors, which might be relevant for treatment with targeted therapy of those patients.^{15-17,19,40,42,43} In our study, we found pRb inactivation in 7/10 patients with combined LCNEC-ADC (*RB1* mutation or loss of pRb expression). The difference between *RB1* mutational status and pRb expression might be explained by production of nonfunctional pRb and by additional mechanisms for pRb inactivation, that is, gene rearrangement, epigenetic inactivation or p16 inactivation.^{15,44} Ito et al found *RB1* mutations in 4/10 cases and loss of pRb expression in 7/10 cases of combined LCNEC-ADC tumors.⁴⁰ In the five LCNEC-ADC cases presented by Miyoshi et al, 1/5 tumors had an *RB1* mutation, but indications for other mechanisms of pRb inactivation were not investigated.¹⁹ Milione et al found *RB1* mutations in only 1/16 tumors and loss of pRb expression in 8/26 tumors; however, only mutations in hotspot areas were analyzed in our study.⁴¹ In all, a frequent inactivation of pRb is found in combined LCNEC-ADC, which is comparable to incidences in general LCNEC.¹⁵⁻¹⁷ However, *RB1* mutations are rare in ADC, and therefore, we would have expected to find a lower percentage of *RB1* mutations, especially in ADC-parts.¹⁰ It has been shown that *RB1* mutations can result in *BRN2* upregulation leading to neuroendocrine differentiation.^{44,45} Apparently, *RB1* inactivation by mutations or other mechanisms have an important role in the development of combined LCNEC-ADC lesions. This is in concordance with *RB1* mutations found in NSCLC tumors with *EGFR* mutations transforming to SCLC or LCNEC during the course of TKI therapy.^{5,6,9,10}

Because we and others found a clonal relationship between LCNEC- and ADC-parts of combined tumors, a common cell of origin

is likely.¹⁹ Presumably, this is a nonneuroendocrine cell, because ADC is known to origin from nonneuroendocrine cells, and development of LCNEC from nonneuroendocrine cells has also been reported in mouse models.^{46,47} Even the two combined LCNEC identified as SCLC-like most likely have a nonneuroendocrine cell of origin, considering the clear nonneuroendocrine morphology of the ADC-part. Immunohistochemistry revealed that the number and intensity of positive neuroendocrine markers and *Ascl1* expression increased comparing pure ADC with combined ADC and combined and pure LCNEC. Furthermore, some combined ADC-parts showed sparse, scattered single cell neuroendocrine marker expression while others had increased expression near the LCNEC-part. This argues for aberrant differentiation in the transition from ADC to LCNEC, in which some of the tumor cells already express neuroendocrine markers, despite conservation of clear morphological characteristics of ADC. Theoretically, it could also be possible that LCNEC tumors differentiate to ADC. However, this is less likely due to the less aggressive behavior of NSCLC compared with LCNEC, as is also reflected by the trend toward a lower median Ki-67 proliferation index in ADC-parts compared with LCNEC-parts of combined tumors in our study. Furthermore, temporal transformation of LCNEC towards ADC during active treatment has never been reported, in contrast to the cases of transformation from ADC to LCNEC during TKI treatment.³⁻⁵ Nowadays, tumors with nonsmall cell, nonneuroendocrine morphology but with positive staining of neuroendocrine markers are regarded as “NSCLC with neuroendocrine differentiation” and treated as NSCLC.¹⁴ However, those tumors might resemble ADC-parts of the combined tumors. Relevance of this neuroendocrine profile in ADC has been shown previously by inferior survival in *Ascl1*+ ADC patients and ADC patients with an *Ascl1*-associated gene expression signature.⁴⁸⁻⁵⁰ It is tempting to speculate that ADC tumors with expression of *Ascl1* or neuroendocrine markers are also a reflection of an aberrant differentiation process from ADC to LCNEC. Further studies should focus on morphological, histological, mutational and clinical features of these special tumors to evaluate clinical relevance.

A couple of molecular mechanisms have been reported possibly underlying development of neuroendocrine differentiation in tumors, for example, pRb inactivation, *Ascl1* upregulation or *Rest* downregulation.^{44,45,51-53} We found *RB1* mutations and homozygous deletions or loss of functional pRb that might have been the trigger for neuroendocrine differentiation in Patients 1, 3, 5, 7, 8, 9 and 13. In the LCNEC-part of the combined tumor of Patient 2, *Ascl1* was upregulated and *Rest* downregulated, which might explain neuroendocrine differentiation in this part of the tumor. In Patients 4 and 14, neuroendocrine differentiation might have been driven by *Ascl1* upregulation, which was already present in the ADC-parts of both tumors. Whether or not the expression of *Ascl1* is the result of another underlying mechanism driving neuroendocrine differentiation (eg, Notch1 silencing) remains to be studied.⁵⁴⁻⁵⁷ In SCLC expression of the transcriptional regulator, *NeuroD1* is an important feature in a subgroup of patients.⁵⁸ However, we did not find a difference in *NeuroD1* expression between ADC-parts and LCNEC-parts of

combined tumors, and therefore, *NeuroD1* seems not to have an obvious regulatory role in these combined LCNEC-ADC tumors.

In contrast to high clonality found in combined tumors, clonality existed in only one out of five sets of co-primary LCNEC and ADC tumors. For this case (Patient 13) with combined LCNEC-ADC and ipsilateral co-primary ADC, management or the staging category (IIIA) was not impacted in retrospect. A clonal relationship was demonstrated before in co-primary NSCLC lesions (mainly ADC) with different morphologic subtypes by evaluation of 20 lung cancer genes, but a clonal relationship has never been reported for co-primary tumors including LCNEC.^{36,37} Therefore, staging of co-primary tumors remains a delicate matter, and mutational analysis could be used to evaluate clonal relationship when considered crucial for staging and treatment decisions.

In our study, we could only include 10 combined lesions and 5 patients with co-primary tumors, identified from a dataset of 305 resected LCNEC cases in the Netherlands. The main reason for the low percentage of included patients compared with other studies is the very strict criteria we used to select a homogeneous population to secure the quality of the study.^{18,19} We only selected combined LCNEC-ADC cases and excluded cases with squamous cell carcinoma, since more is known about targetable mutations and transformation to neuroendocrine carcinomas under the course of therapy in ADC. Furthermore, we restricted selection to cases with adequately distinguishable parts of ADC and LCNEC, both sufficient for microdissection of DNA. Tumors with solely intermingled parts and tumors with amphicrine cells were not included.

In conclusion, our data indicate that combined tumors with LCNEC- and ADC-parts, identifiable according to WHO criteria, are clonally related, with a high rate of mutations frequently encountered in pure ADC but also pRb inactivation, associated with neuroendocrine differentiation. This finding points to a common cell of origin of both histologically different neoplastic lesions. Co-primary, but separate LCNEC and ADC tumors were in all but one case not clonally related, indicating that these tumors should be regarded as two primary lesions instead of metastatic disease. In these cases, clonality analysis should be used if considered crucial for staging and treatment decisions.

CONFLICT OF INTEREST

All conflicts disclosed are outside the study. Bregtje C. M. Hermans reports grants from Bristol-Myers Squibb, nonfinancial support from Abbvie; Jules L. Derks reports grants from Bristol-Myers Squibb, nonfinancial support from Abbvie, personal fees from BMS, personal fees from Pfizer, personal fees from Boehringer-Ingelheim, personal fees from Novartis, personal fees from Ipsen; Jan H. von der Thüsen reports personal fees from Roche, Roche Diagnostics, Bristol-Myers Squibb, Eli Lilly, MSD and grants from Bristol-Myers Squibb and AstraZeneca; Wim Timens reports fees to Institution (UMCG) from Roche Diagnostics/Ventana, Merck Sharp Dohme, Bristol-Myers Squibb and AbbVie; Winand N. M. Dinjens reports personal fees from Amgen, Bayer, Bristol-Myers Squibb, Novartis and Roche, laboratory research fees from AstraZeneca, Bristol-Myers Squibb and Abbvie;

Hendrikus J. Dubbink reports grants, personal fees and nonfinancial support from AstraZeneca, personal fees from AbbVie, Bayer, Janssen, Pfizer and Lilly, nonfinancial support from Illumina, grants from Merck; Ernst-Jan M. Speel reports grants from AstraZeneca, Pfizer, Novartis and Bayer, personal fees from Amgen, Lilly and Novartis, nonfinancial support from Abbvie and Biocartis; Anne-Marie C. Dingemans attended advisory boards and/or provided lectures for Roche, BMS, Eli Lilly, Takeda, Boehringer Ingelheim, Astra Zeneca, Pfizer, BMS, Amgen, Novartis, MSD and Pharmamar. She received research support from Amgen. All paid to the institute. The other authors did not report conflicts of interest.

DATA AVAILABILITY STATEMENT

The data that support the findings of our study are available from the corresponding author upon reasonable request.

ETHICS STATEMENT

Our study has been approved by the Medical Ethical Committee of Maastricht UMC+ (14-4-034.8/ab) and was performed according to the regulations as defined by the 'Dutch Federal, Human Tissue and Medical Research: Code of conduct for responsible use (2011)', not requiring patient informed consent.

ORCID

Bregtje C. M. Hermans  <https://orcid.org/0000-0003-4831-3690>

TWITTER

Anne-Marie C. Dingemans  @Dingemans_AnneM

REFERENCES

- Sholl LM, Aisner DL, Varella-Garcia M, et al. Multi-institutional oncogenic driver mutation analysis in lung adenocarcinoma: the lung cancer mutation consortium experience. *J Thorac Oncol.* 2015;10:768-777.
- Grosse A, Grosse C, Rechsteiner M, Soltermann A. Analysis of the frequency of oncogenic driver mutations and correlation with clinicopathological characteristics in patients with lung adenocarcinoma from Northeastern Switzerland. *Diagn Pathol.* 2019;14:18.
- Kogo M, Shimizu R, Uehara K, et al. Transformation to large cell neuroendocrine carcinoma as acquired resistance mechanism of EGFR tyrosine kinase inhibitor. *Lung Cancer.* 2015;90:364-368.
- Baglivo S, Ludovini V, Sidoni A, et al. Large cell neuroendocrine carcinoma transformation and EGFR-T790M mutation as coexisting mechanisms of acquired resistance to EGFR-TKIs in lung cancer. *Mayo Clin Proc.* 2017;92:1304-1311.
- Marcoux N, Gettinger SN, O'Kane G, et al. EGFR-mutant adenocarcinomas that transform to small-cell lung cancer and other neuroendocrine carcinomas: clinical outcomes. *J Clin Oncol.* 2019;37:278-285.
- Niederst MJ, Sequist LV, Poirier JT, et al. RB loss in resistant EGFR mutant lung adenocarcinomas that transform to small-cell lung cancer. *Nat Commun.* 2015;6:6377.
- Garraway LA, Janne PA. Circumventing cancer drug resistance in the era of personalized medicine. *Cancer Discov.* 2012;2:214-226.
- Wu SG, Shih JY. Management of acquired resistance to EGFR TKI-targeted therapy in advanced non-small cell lung cancer. *Mol Cancer.* 2018;17:38.
- Offin M, Chan JM, Tenet M, et al. Concurrent RB1 and TP53 alterations define a subset of EGFR-mutant lung cancers at risk for histologic transformation and inferior clinical outcomes. *J Thorac Oncol.* 2019;14:1784-1793.
- Lee JK, Lee J, Kim S, et al. Clonal history and genetic predictors of transformation into small-cell carcinomas from lung adenocarcinomas. *J Clin Oncol.* 2017;35:3065-3074.
- Derks JL, Hendriks LE, Buikhuisen WA, et al. Clinical features of large cell neuroendocrine carcinoma: a population-based overview. *Eur Respir J.* 2016;47:615-624.
- Korse CM, Taal BG, van Velthuysen ML, Visser O. Incidence and survival of neuroendocrine tumours in the Netherlands according to histological grade: experience of two decades of cancer registry. *Eur J Cancer.* 2013;49:1975-1983.
- Takei H, Asamura H, Maeshima A, et al. Large cell neuroendocrine carcinoma of the lung: a clinicopathologic study of eighty-seven cases. *J Thorac Cardiovasc Surg.* 2002;124:285-292.
- Travis WD, Brambilla E, Burke AP, Markx A, Nicholson AG. *WHO Classification of Tumours of the Lung, Pleura, Thymus and Heart.* Vol 7. 4th ed. Lyon, France: International Agency for Research on Cancer; 2015.
- Derks JL, Leblay N, Thunnissen E, et al. Molecular subtypes of pulmonary large-cell neuroendocrine carcinoma predict chemotherapy treatment outcome. *Clin Cancer Res.* 2018;24:33-42.
- George J, Walter V, Peifer M, et al. Integrative genomic profiling of large-cell neuroendocrine carcinomas reveals distinct subtypes of high-grade neuroendocrine lung tumors. *Nat Commun.* 2018;9:1048.
- Rekhtman N, Pietanza MC, Hellmann MD, et al. Next-generation sequencing of pulmonary large cell neuroendocrine carcinoma reveals small cell carcinoma-like and non-small cell carcinoma-like subsets. *Clin Cancer Res.* 2016;22:3618-3629.
- Asamura H, Kameya T, Matsuno Y, et al. Neuroendocrine neoplasms of the lung: a prognostic spectrum. *J Clin Oncol.* 2006;24:70-76.
- Miyoshi T, Umemura S, Matsumura Y, et al. Genomic profiling of large-cell neuroendocrine carcinoma of the lung. *Clin Cancer Res.* 2017;23:757-765.
- Zhang JT, Li Y, Yan LX, et al. Disparity in clinical outcomes between pure and combined pulmonary large-cell neuroendocrine carcinoma: a multi-center retrospective study. *Lung Cancer.* 2020;139:118-123.
- Buys TP, Aviel-Ronen S, Waddell TK, Lam WL, Tsao MS. Defining genomic alteration boundaries for a combined small cell and non-small cell lung carcinoma. *J Thorac Oncol.* 2009;4:227-239.
- Rekhtman N, Borsu L, Reva B, et al. Unsuspected collision of synchronous lung adenocarcinomas: a potential cause of aberrant driver mutation profiles. *J Thorac Oncol.* 2014;9:e1-e3.
- Lin MW, Su KY, Su TJ, et al. Clinicopathological and genomic comparisons between different histologic components in combined small cell lung cancer and non-small cell lung cancer. *Lung Cancer.* 2018;125:282-290.
- Wagner PL, Kitabayashi N, Chen YT, Saqi A. Combined small cell lung carcinomas: genotypic and immunophenotypic analysis of the separate morphologic components. *Am J Clin Pathol.* 2009;131:376-382.
- Zhao X, McCutcheon JN, Kallakury B, et al. Combined small cell carcinoma of the lung: is it a single entity? *J Thorac Oncol.* 2018;13:237-245.
- Mascalchi M, Comin CE, Bertelli E, et al. Screen-detected multiple primary lung cancers in the ITALUNG trial. *J Thorac Dis.* 2018;10:1058-1066.
- Lv J, Zhu D, Wang X, Shen Q, Rao Q, Zhou X. The value of prognostic factors for survival in synchronous multifocal lung cancer: a retrospective analysis of 164 patients. *Ann Thorac Surg.* 2018;105:930-936.
- Liu M, He W, Yang J, Jiang G. Surgical treatment of synchronous multiple primary lung cancers: a retrospective analysis of 122 patients. *J Thorac Dis.* 2016;8:1197-1204.
- Hsu HH, Ko KH, Chou YC, et al. SUVmax and tumor size predict surgical outcome of synchronous multiple primary lung cancers. *Medicine (Baltimore).* 2016;95:e2351.

30. Arai J, Tsuchiya T, Oikawa M, et al. Clinical and molecular analysis of synchronous double lung cancers. *Lung Cancer*. 2012;77:281-287.
31. Yu YC, Hsu PK, Yeh YC, et al. Surgical results of synchronous multiple primary lung cancers: similar to the stage-matched solitary primary lung cancers? *Ann Thorac Surg*. 2013;96:1966-1974.
32. Roepman P, Ten Heuvel A, Scheidel KC, et al. Added value of 50-gene panel sequencing to distinguish multiple primary lung cancers from pulmonary metastases: a systematic investigation. *J Mol Diagn*. 2018;20:436-445.
33. Yamada Y, Iyoda A, Suzuki M, et al. Double primary lung carcinoma consisting of large cell neuroendocrine carcinoma and squamous cell carcinoma: report of a case. *Ann Thorac Cardiovasc Surg*. 2005;11:397-400.
34. Kashif M, Ayyadurai P, Thanha L, Khaja M. Triple synchronous primary lung cancer: a case report and review of the literature. *J Med Case Reports*. 2017;11:245.
35. Detterbeck FC, Franklin WA, Nicholson AG, et al. The IASLC lung cancer staging project: background data and proposed criteria to distinguish separate primary lung cancers from metastatic foci in patients with two lung tumors in the forthcoming eighth edition of the TNM classification for lung cancer. *J Thorac Oncol*. 2016;11:651-665.
36. Takahashi Y, Shien K, Tomida S, et al. Comparative mutational evaluation of multiple lung cancers by multiplex oncogene mutation analysis. *Cancer Sci*. 2018;109:3634-3642.
37. Murphy SJ, Harris FR, Kosari F, et al. Using genomics to differentiate multiple primaries from metastatic lung cancer. *J Thorac Oncol*. 2019;14:1567-1582.
38. Casparie M, Tiebosch AT, Burger G, et al. Pathology databanking and biobanking in the Netherlands, a central role for PALGA, the nationwide histopathology and cytopathology data network and archive. *Cell Oncol*. 2007;29:19-24.
39. Dubbink HJ, Atmodimedjo PN, van Marion R, et al. Diagnostic detection of allelic losses and imbalances by next-generation sequencing: 1p/19q co-deletion analysis of gliomas. *J Mol Diagn*. 2016;18:775-786.
40. Ito M, Miyata Y, Hirano S, et al. Therapeutic strategies and genetic profile comparisons in small cell carcinoma and large cell neuroendocrine carcinoma of the lung using next-generation sequencing. *Oncotarget*. 2017;8:108936-108945.
41. Milione M, Maisonneuve P, Grillo F, et al. Ki-67 index of 55% distinguishes two groups of bronchopulmonary pure and composite large cell neuroendocrine carcinomas with distinct prognosis. *Neuroendocrinology*. 2021;111(5):475-489.
42. Planchard D, Popat S, Kerr K, et al. Metastatic non-small cell lung cancer: ESMO Clinical Practice Guidelines for diagnosis, treatment and follow-up. *Ann Oncol*. 2018;29:iv192-iv237.
43. Lanman BA, Allen JR, Allen JG, et al. Discovery of a covalent inhibitor of KRAS(G12C) (AMG 510) for the treatment of solid tumors. *J Med Chem*. 2020;63:52-65.
44. Gouyer V, Gazzeri S, Bolon I, Drevet C, Brambilla C, Brambilla E. Mechanism of retinoblastoma gene inactivation in the spectrum of neuroendocrine lung tumors. *Am J Respir Cell Mol Biol*. 1998;18:188-196.
45. Cobrinik D, Francis RO, Abramson DH, Lee TC. Rb induces a proliferative arrest and curtails Brn-2 expression in retinoblastoma cells. *Mol Cancer*. 2006;5:72.
46. Derks JL, Leblay N, Lantuejoul S, Dingemans AC, Speel EM, Fernandez-Cuesta L. New insights into the molecular characteristics of pulmonary carcinoids and large cell neuroendocrine carcinomas, and the impact on their clinical management. *J Thorac Oncol*. 2018;13:752-766.
47. Lazaro S, Perez-Crespo M, Lorz C, et al. Differential development of large-cell neuroendocrine or small-cell lung carcinoma upon inactivation of 4 tumor suppressor genes. *Proc Natl Acad Sci U S A*. 2019;116:22300-22306.
48. Kosari F, Ida CM, Aubry MC, et al. ASCL1 and RET expression defines a clinically relevant subgroup of lung adenocarcinoma characterized by neuroendocrine differentiation. *Oncogene*. 2014;33:3776-3783.
49. Augustyn A, Borromeo M, Wang T, et al. ASCL1 is a lineage oncogene providing therapeutic targets for high-grade neuroendocrine lung cancers. *Proc Natl Acad Sci U S A*. 2014;111:14788-14793.
50. Miyashita N, Horie M, Suzuki HI, et al. An integrative analysis of transcriptome and epigenome features of ASCL1-positive lung adenocarcinomas. *J Thorac Oncol*. 2018;13:1676-1691.
51. Kreisler A, Strissel PL, Strick R, Neumann SB, Schumacher U, Becker CM. Regulation of the NRSF/REST gene by methylation and CREB affects the cellular phenotype of small-cell lung cancer. *Oncogene*. 2010;29:5828-5838.
52. Kunnimalaiyaan M, Chen H. Tumor suppressor role of Notch-1 signaling in neuroendocrine tumors. *Oncologist*. 2007;12:535-542.
53. Kudoh S, Tenjin Y, Kameyama H, et al. Significance of achaete-scute complex homologue 1 (ASCL1) in pulmonary neuroendocrine carcinomas; RNA sequence analyses using small cell lung cancer cells and Ascl1-induced pulmonary neuroendocrine carcinoma cells. *Histochem Cell Biol*. 2020;153:443-456.
54. Henke RM, Meredith DM, Borromeo MD, Savage TK, Johnson JE. Ascl1 and Neurog2 form novel complexes and regulate Delta-like3 (Dll3) expression in the neural tube. *Dev Biol*. 2009;328:529-540.
55. Jiang T, Collins BJ, Jin N, et al. Achaete-scute complex homologue 1 regulates tumor-initiating capacity in human small cell lung cancer. *Cancer Res*. 2009;69:845-854.
56. Linnoila RI, Zhao B, DeMayo JL, et al. Constitutive achaete-scute homologue-1 promotes airway dysplasia and lung neuroendocrine tumors in transgenic mice. *Cancer Res*. 2000;60:4005-4009.
57. Hassan WA, Takebayashi SI, Abdalla MOA, et al. Correlation between histone acetylation and expression of Notch1 in human lung carcinoma and its possible role in combined small-cell lung carcinoma. *Lab Invest*. 2017;97:913-921.
58. Rudin CM, Poirier JT, Byers LA, et al. Molecular subtypes of small cell lung cancer: a synthesis of human and mouse model data. *Nat Rev Cancer*. 2019;19:289-297.

SUPPORTING INFORMATION

Additional supporting information may be found in the online version of the article at the publisher's website.

How to cite this article: Hermans BCM, Derks JL, Hillen LM, et al. In-depth molecular analysis of combined and co-primary pulmonary large cell neuroendocrine carcinoma and adenocarcinoma. *Int. J. Cancer*. 2022;150(5):802-815. doi:10.1002/ijc.33853